Carbon cost of plant nitrogen acquisition: global carbon cycle impact from an improved plant nitrogen cycle in the Community Land Model

MINGJIE SHI[1,2], JOSHUA B. FISHER[1,2], EDWARD R. BRZOSTEK[3] and RICHARD P. PHILLIPS[4]

[1]*Jet Propulsion Laboratory, California Institute of Technology, 4800 Oak Grove Drive, Pasadena, CA 91109, USA,* [2]*Joint Institute for Regional Earth System Science and Engineering, University of California at Los Angeles, Los Angeles, CA 90095, USA,* [3]*Department of Biology, West Virginia University, 53 Campus Drive, Morgantown, WV 26506, USA,* [4]*Department of Biology, Indiana University, 702 N. Walnut Grove Avenue, Bloomington, IN 47405, USA*

Abstract

Plants typically expend a significant portion of their available carbon (C) on nutrient acquisition – C that could otherwise support growth. However, given that most global terrestrial biosphere models (TBMs) do not include the C cost of nutrient acquisition, these models fail to represent current and future constraints to the land C sink. Here, we integrated a plant productivity-optimized nutrient acquisition model – the Fixation and Uptake of Nitrogen Model – into one of the most widely used TBMs, the Community Land Model. Global plant nitrogen (N) uptake is dynamically simulated in the coupled model based on the C costs of N acquisition from mycorrhizal roots, nonmycorrhizal roots, N-fixing microbes, and retranslocation (from senescing leaves). We find that at the global scale, plants spend 2.4 Pg C yr^{-1} to acquire 1.0 Pg N yr^{-1}, and that the C cost of N acquisition leads to a downregulation of global net primary production (NPP) by 13%. Mycorrhizal uptake represented the dominant pathway by which N is acquired, accounting for ~66% of the N uptake by plants. Notably, roots associating with arbuscular mycorrhizal (AM) fungi – generally considered for their role in phosphorus (P) acquisition – are estimated to be the primary source of global plant N uptake owing to the dominance of AM-associated plants in mid- and low-latitude biomes. Overall, our coupled model improves the representations of NPP downregulation globally and generates spatially explicit patterns of belowground C allocation, soil N uptake, and N retranslocation at the global scale. Such model improvements are critical for predicting how plant responses to altered N availability (owing to N deposition, rising atmospheric CO_2, and warming temperatures) may impact the land C sink.

Keywords: carbon cost, Community Land Model, Fixation and Uptake of Nitrogen, mycorrhizal fungi, nitrogen uptake, net primary production

Received 23 May 2015 and accepted 28 September 2015

Introduction

Terrestrial biosphere models (TBMs) simulate the response of the terrestrial carbon (C) source/sink dynamics to global change (Huntzinger *et al.*, 2013; Fisher *et al.*, 2014; Zaehle *et al.*, 2014). Given that recent empirical evidence has reaffirmed the role of nutrient availability in regulating net ecosystem production and ecosystem C use efficiency at the global scale (Fisher *et al.*, 2012; Fernández-Martínez *et al.*, 2014), accurate predictions of the land C sink in the future rely on how well TBMs capture nutrient constraints (Wieder *et al.*, 2015). Many TBMs now include some representation of the nitrogen (N) cycle, reflecting the importance of N as the primary limiting nutrient across much of the Earth's land surface (Vitousek & Howarth, 1991; Lebauer & Treseder, 2008). In the latest Multi-scale Synthesis and Terrestrial Model Intercomparison Project (MsTMIP), 12 of 22 models included some representation of how N constrains primary production (Huntzinger *et al.*, 2013). However, all of these models assume that N is acquired at no C cost to plants. This directly contradicts empirical evidence from individual plants that shows that nearly every pathway by which a plant acquires N requires a significant amount of energy; energy that would otherwise be allocated as C to aboveground growth. Thus, by omitting the C cost of N acquisition, TBMs fail to capture a critical coupling of the C and N cycles and as a consequence likely overestimate the size and dynamic N-sensitivity of the land C sink (Ostle *et al.*, 2009; Fisher *et al.*, 2010).

The energy or C costs for N acquisition come from resorbing N from senescing leaves, fixing N_2 gas into biological reactive forms, or mobilizing and taking up N that is locked in soil solution or organic matter (Vitousek & Field, 1999; Rastetter *et al.*, 2001; Dickinson

Correspondence: Joshua B. Fisher, tel. +1 818 354 0934, fax +1 818 354 9476, e-mail: joshua.b.fisher@jpl.nasa.gov

et al., 2002; Vitousek *et al.*, 2002; Wang *et al.*, 2007). While it is well-known that plants allocate C to acquire N from more than one pathway, few studies have quantified the variable costs of mobilizing N from each pathway, or the degree to which such costs differ dynamically within and among ecosystems. For example, while trees allocate up to 20% of net primary production (NPP) to both symbiotic and free-living microbes at the root surface to increase their access to N (Högberg & Högberg, 2002; Hobbie, 2006; Brzostek *et al.*, 2015), the amount of C allocated to N uptake from fixation vs. mycorrhizal uptake can vary by a factor of two depending on stand age, soil fertility, or the dominant tree species (Brzostek *et al.*, 2014). Moreover, as the availability of N in a given ecosystem declines, the C costs of taking up N increases, leading to a smaller return of N per unit C invested (Fisher *et al.*, 2010; Brzostek *et al.*, 2014). Thus, 'N-limitation' is a function of two dynamics: (i) minimal N available in the soil; or, (ii) available N, but not enough C to acquire it. Most TBMs are missing the second dynamic (Thornton *et al.*, 2007, 2009; Ostle *et al.*, 2009).

To account for the lack of a C cost to N acquisition in TBMs, Fisher *et al.* (2010) developed the Fixation and Uptake of Nitrogen (FUN) model. FUN is grounded in optimal allocation theory whereby plants optimize the allocation of C used to acquire N from the soil (directly through roots or from mycorrhizal symbionts), senescing leaves, and symbiotic biological N fixation (BNF) to maximize growth (Bloom *et al.*, 1985; Rastetter *et al.*, 1997). In contrast to other efforts, FUN was explicitly developed to be coupled into TBMs and as a result it has relatively few required model inputs (e.g., temperature, NPP, and leaf N) and parameters. FUN is also highly modular leading to rapid model development. Brzostek *et al.* (2014) showed that integrating C–N trade-offs between the two major types of fungi that plants associate with – arbuscular mycorrhizal (AM) or ectomycorrhizal (ECM) fungi – into FUN2.0 improved the dynamic predictions of the N retranslocated from leaves and taken up from the soil. While these improvements were validated against six forested sites (including four experimental free air CO$_2$ enrichment or FACE sites), the global implications on the land C sink remain to be tested.

Here, we coupled FUN2.0 into the Community Land Model version 4.0 (CLM4.0) to examine the sensitivity of the land C sink to a dynamic C cost of N acquisition that varies across plant functional types (PFTs). We evaluated modern era global model runs to address the following questions in the updated model: (i) Which ecosystems take up the most N and which are the most N-limited? (ii) How does the C cost of N acquisition vary spatially and temporally? (iii) How sensitive is the land C sink to a dynamic prediction of the C cost of N acquisition?

Materials and methods

Model description

Fixation and Uptake of Nitrogen is a mathematical and computational model of plant N acquisition (Fisher *et al.*, 2010). In the original FUN1.0, plants obtain N through the following pathways: (i) passive uptake, (ii) active uptake, (iii) retranslocation, and (iv) symbiotic BNF, which are briefly described here (see Fisher *et al.*, 2010 for full model description). Passive uptake refers to plants taking up soluble N through the transpiration stream at no C cost to the plant. It varies as a function of transpiration rates and the amount of mineral N dissolved in the soil. Active N uptake encapsulates the energy needed to move N into root cells and the C expended into the soil to prime nutrient mobilization from soil organic matter (SOM). The C spent on active N uptake decreases as root biomass or soil N availability increase. Retranslocation is the N resorption in leaves before senescence (Fisher *et al.*, 2010); N resorption needs C to synthesize the enzymes and regulatory elements and to drive the translocation stream (Holopainen & Peltonen, 2002; Wright & Westoby, 2003). The cost of retranslocation is modeled to increase as leaf N decreases (Brzostek *et al.*, 2014). Symbiotic BNF is the process by which atmospheric N is converted into ammonium. The cost of symbiotic BNF is modeled to vary as a function of temperature based on empirical relationships between temperature and nitrogenase activity (Houlton *et al.*, 2008).

The modularity of FUN allows it to be easily modified. FUN2.0 (Brzostek *et al.*, 2014) included two main improvements: (i) integrated trade-offs between ECM, AM, and nonmycorrhizal roots in their C costs of N acquisition and (ii) a resistance network to allow simultaneous uptake across all pathways (Fig. 1). In FUN2.0, when soil N is relatively abundant, plants supporting AM have the lowest C costs; when soil N is limiting, plants supporting ECM have the most optimal strategy. At extremely high levels of soil N (i.e., at the level of fertilized agricultural fields), passive and nonmycorrhizal root uptake dominates (Cai *et al.*, 2015). Each pathway occupies positions in the root biomass and N availability space where it is the optimal strategy for taking up N from the soil. Both Fisher *et al.* (2010) and Brzostek *et al.* (2014) stated an assumed nonpreference for the uptake of ammonium (NH$_4^+$) and nitrate (NO$_3^-$) in the two FUN model versions, as it is still unclear how generalizable plant preference for uptake of NH$_4^+$, NO$_3^-$, and dissolved organic N is at the global scale (Falkengren-Grerup, 1995; Marschner, 1995; Nordin *et al.*, 2001; Jones *et al.*, 2005).

The full TBM used in this study is CLM4.0 (Oleson *et al.*, 2010; Lawrence *et al.*, 2011), which is the land component of the Community Earth System Model (CESM) (Gent *et al.*, 2011). Specifically, we use CLM4.0 with C and N dynamics (i.e., CLM4.0CN), which was originally developed by integrating the Biome-BGC model (Thornton *et al.*, 2002) into CLM version 3.0 (Oleson *et al.*, 2004; Bonan & Levis, 2006; Dickinson
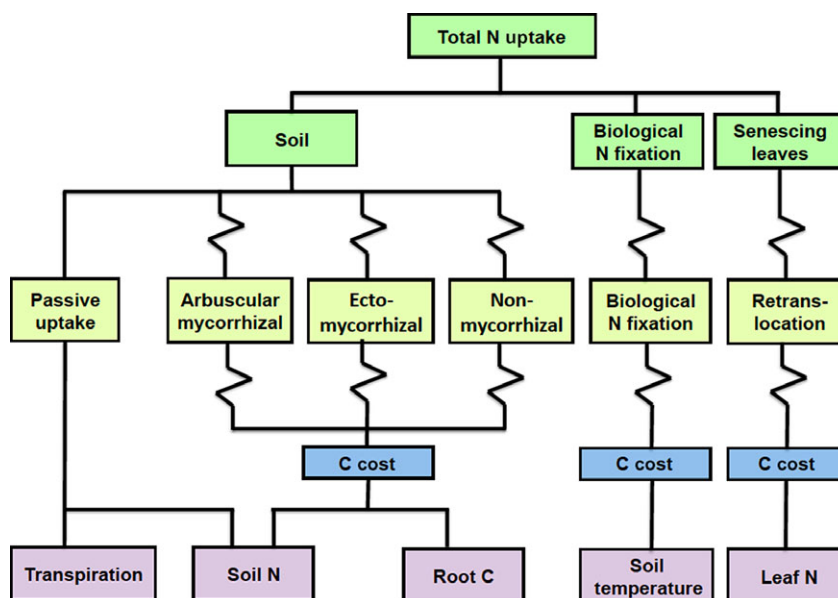
Fig. 1 The schematic diagram of FUN2.0.

et al., 2006); N dynamics are only in the soil processes – plant N dynamics outside of stoichiometric constraints are missing. Leaf, respiring, and nonrespiring woody components of stems and coarse roots, and fine roots are the structural vegetation pools of CLM4.0. CLM4.0 reserves C and N obtained in one growing season in storage pools and distributes these reserves as new structural growth in the following year (Thornton & Zimmermann, 2007). A coarse woody debris pool, three litter pools, and four SOM pools, representing C and N storage and fluxes, are arranged as a converging trophic decomposition cascade (Thornton & Rosenbloom, 2005; Shi et al., 2013).

Coupling FUN2.0 to CLM4.0

FUN2.0 uses ten input variables (Table 1). Most of the variables including available soil N (N_{soil}), fine root biomass (C_{root}), leaf N before senescence (N_{leaf}), NPP (C_{NPP}), soil water depth (S_d), soil temperature (T_{soil}), and transpiration (E_T) are directly calculated by the C–N processes of CLM4.0. This section explains how we derived or directly used variables from CLM4.0 to generate the necessary inputs for FUN2.0 as well as the key modifications needed to enable the coupling between FUN and CLM.

In CLM4.0, plant N uptake has two pathways, which are modeled as soil N uptake and retranslocation (Oleson et al., 2010). Soil N uptake requires no C expenditure and depends on the concentration of mineral N in the soil, and the relative demand of microbes and plants for the available N. Retranslocation is set at a fixed rate of 50% varying in absolute amount based on the product of leaf litter C and fixed C : N ratios of leaves and leaf litter (Appendix S1). When soil mineral N cannot meet ecosystem N demand, which is equal to the sum of plant and microbial N demand for N, the amount of soil N available to plants is reduced based

upon the actual N immobilized by soil microbes. Otherwise, all of the available soil N is taken up at no cost to meet plant N demand. The available soil N that takes into account microbial immobilization represents the plant available N to FUN2.0 (i.e., N_{soil}). To calculate the whole plant C : N ratio input (i.e., $R_{C : N}$), we divided the total C in leaves, fine roots, live coarse roots, and live stems by the total N in the same components of the plant.

To generate the trade-offs between ECM, AM, and nonmycorrhizal root uptake, FUN2.0 needs an estimate of the percentage of aboveground biomass that associates with each mycorrhizal type for each pixel (Brzostek et al., 2014). For each PFT, we classified them based upon known associations between the plant species and either AM- and ECM-fungi. This results in some PFTs being largely AM-dominated (e.g., grasslands, crops) and some being largely ECM-dominated (e.g., boreal forest) (Read, 1991; Allen et al., 1995; Phillips et al., 2013). We acknowledge that these PFT fractions are coarse and do not capture the spatial heterogeneity in mycorrhizal association that is present across the landscape, particularly in mixed-mycorrhizal PFTs, such as tropical (Waring et al., 2015) and temperate forests (Phillips et al., 2013). In addition, we are transparent in our reporting of the results to highlight how this coarse classification impacts our results. Based on the discussion above, the fractions of the AM- and ECM-associated plants were derived and then applied to each of the CLM4.0 PFT category (Table 2) by multiplying the land cover fraction of each PFT. At the same time, available C, leaf N, and root C are separated between the AM and the ECM portion of each PFT based upon these percentages. This new coupled model structure allows the parallelized calculations of N uptake pathways across the AM and ECM fractions of a given PFT in each pixel. With certain amounts of soil N and root C, the C cost and N acquisition amount are different for AM- and ECM-associated PFTs (Soudzilovskaia et al., 2015). Therefore,

Table 1 The input parameters of FUN 2.0 (Brzostek *et al.*, 2014)

Parameters	Notation	Units in FUN2.0	Units in CLM4.0–FUN2.0
Available soil N	N_{soil}	kg N m^{-2}	g N m^{-2}
Fine root biomass	C_{root}	kg C m^{-2}	g C m^{-2}
Leaf N before senescence	N_{leaf}	kg N m^{-2}	g N m^{-2}
Net primary production	C_{NPP}	kg C m^{-2} yr^{-1}	g C m^{-2} yr^{-1}
Soil water depth	S_d	m	m
Soil temperature	T_{soil}	^oC	Kelvin
Transpiration	E_T	m s^{-1}	mm s^{-1}
Plant C : N ratio	$R_{C:N}$	kg C kg N^{-1}	g C g N^{-1}
Percent ECM basal area	%ECM	Unitless	Unitless
Ability to fix	A_{fix}	TRUE or FALSE	TRUE or FALSE

Table 2 The ratios of the arbuscular mycorrhizal (AM)-associated and ectomycorrhizal (ECM)-associated plants of the CLM4.0 PFTs

Name of the PFTs	AM (%)	ECM (%)
Bare soil (not vegetated)	0	100
Needleleaf evergreen temperate tree	0	100
Needleleaf evergreen boreal tree	0	100
Needleleaf deciduous boreal tree	0	100
Broadleaf evergreen tropical tree	100	0
Broadleaf evergreen temperate tree	100	0
Broadleaf deciduous tropical tree	100	0
Broadleaf deciduous temperate tree	50	50
Broadleaf deciduous boreal tree	0	100
Broadleaf evergreen shrub	0	100
Broadleaf deciduous temperate shrub	0	100
Broadleaf deciduous boreal shrub	0	100
C3 arctic grass	0	100
C3 nonarctic grass	100	0
C4 grass	100	0
Corn	100	0
Wheat	100	0

the mycorrhizal root uptake amount (i.e., the total of AM- and ECM-associated N uptake) and its distribution are given in Table 2. Finally, the C available to allocate to either growth or N uptake is calculated as the difference between gross primary productivity (GPP) and plant maintenance respiration in each pixel and fraction.

In CLM4.0, plant N demand is driven entirely by GPP and the stoichiometry of the tissues where the assimilated C is allocated. Thus, in ecosystems dominated by deciduous plants, there is no N demand (and subsequently no N retranslocation) prior to leaf senescence (Duchesne *et al.*, 2001). In general, CLM4.0 has three broad phenological types: an evergreen type, a seasonal-deciduous type, and a stress-deciduous type. Given the lack of a mismatch between senescence and N demand in evergreen systems, it was not necessary to alter the plant N demand structure. However, to dynamically predict retranslocation in seasonal-deciduous and stress-deciduous systems, it was necessary to alter the timing of N demand. To do this, we used CLM4.0 to estimate plant N demand, which is called N_{demand}, and included a N demand pool specifically during the senescence period in deciduous PFTs (herein $N_{demand\_retransn}$). The annual size of $N_{demand\_retransn}$ is equal to the total amount of stored N that is mobilized to support leaf development during the spring. Due to the lack of C available directly from assimilation during this period, stored C in the leaf C storage pool is used to support uptake in the model. Thus, the sum of N_{demand} and $N_{demand\_retransn}$ is used as the full N demand of the plants in the coupled model and is integrated into all of the FUN2.0 optimization equations.

We have named the coupled model as CLM4.0CN-FUN2.0, and we refer to henceforth as CLM4.0–FUN2.0. The fully coupled model simulates soil N uptake across all of the FUN2.0 pathways: passive uptake, mycorrhizal root uptake, nonmycorrhizal root uptake, and symbiotic BNF. The dynamically predicted soil N uptake as well as retranslocation replaces the more fixed estimates simulated by CLM4.0. On each model time step, the model optimally allocates C to growth as well as the C spent on acquiring N from soil, leaves, and symbiotic BNF. Based on the plant N demand calculated by the algorithm in CLM4.0, the coupled model calculates the C used for N acquisition associated with N_{demand}. The C spent on all active uptake pathways and BNF is respired by soil, which is then added to the soil heterotrophic respiration. The amount of C use based on $N_{demand\_retransn}$ is respired by the plant, which is added to the autotrophic respiration. The total amount of C used to acquire N from the soil, leaves, and air is used to downregulate the NPP of CLM4.0–FUN2.0.

Data description and model settings

The simulation of this study starts with a twentieth-century steady state generated by the National Center for Atmospheric Research (NCAR). We ran the model using meteorological forcing data from Qian *et al.* (2006) and included all the meteorological variables needed by CLM to drive both CLM4.0 and CLM4.0–FUN2.0 at the 0.9° × 1.25° and half-hourly spatiotemporal resolution. Atmospheric N deposition for each model grid cell was obtained from a transient 1850–2009 Community Atmosphere Model (CAM) simulation with interactive chemistry driven by CCSM twentieth-century sea-surface temperatures and emissions (Oleson *et al.*, 2010; Lamarque *et al.*, 2013). We ran the model globally for a 25-year period (1980–2004) and analyzed a 10-year (1995–2004)-period

result. For global validation, we used a new global nutrient limitation product that is derived from remote sensing of evapotranspiration and plant productivity (Fisher *et al.*, 2012) and analyzed whether the downregulation of NPP predicted by CLM4.0–FUN2.0 agreed with this product. However, as we note later in the Discussion, this product includes both N and P limitations, so is not directly comparable to our N-only limitation; we use this product only qualitatively in comparison.

Results

Which ecosystems take up the most N and which are the most N-limited?

Globally, both the amount of N uptake and the pathway of N acquisition varied as a function of ecosystem productivity and dominant mycorrhizal type. CLM4.0–FUN2.0 simulated the mean annual global total N uptake of 1023.9 Tg N yr^{-1}, compared to that simulated by CLM4.0 of 1203.8 Tg N yr^{-1}, a difference of 15%. Global total passive N uptake through the transpiration stream is minor, amounting to 0.7 Tg N

yr^{-1}, which is less than 1% of the global total N uptake (Appendix S2). There were clear patterns in the global distribution of the four major N uptake pathways (Fig. 2). Mycorrhizal root uptake and non-mycorrhizal root uptake have similar global distributions but different magnitudes (Fig. 2a, b), and the spatial correlation coefficient between these two types of uptake amounts is 0.99. The global total mycorrhizal root uptake and the nonmycorrhizal root uptake amounts are 673.6 Tg N yr^{-1} and 103.1 Tg N yr^{-1}, respectively. This reflects the lower C cost of uptake by mycorrhizal roots compared to nonmycorrhizal roots (Brzostek *et al.*, 2014). The tropics, southeast Brazil, southeast USA, and southeast China have the largest soil N uptake rates globally. Boreal forests and tundra ecosystems have the lowest rates of N taken up from the soil (Fig. 2a, b).

When we separated mycorrhizal root uptake into its AM and ECM components, there were clear spatial differences owing to the distribution of AM and ECM abundances in each PFT (Table 2). For example, AM
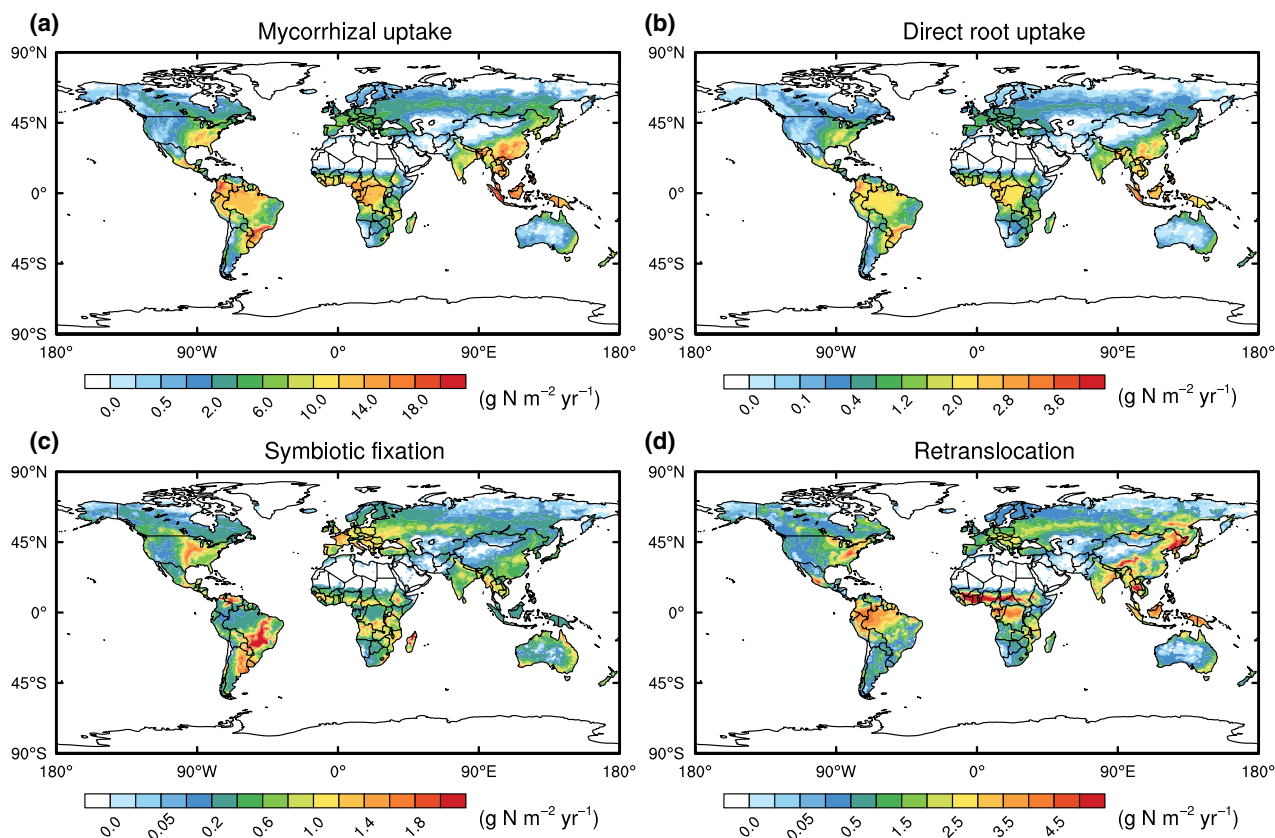

Fig. 2 The global mean annual (1995–2004) (a) mycorrhizal uptake (i.e., mycorrhizal root uptake; mycorrhizal uptake is called in the figures for short), (b) direct root uptake (i.e., nonmycorrhizal root uptake; direct root uptake is called in the figures for short), (c) symbiotic fixation (i.e., symbiotic biological N fixation; symbiotic fixation is called in the figures for short), and (d) retranslocation (g N m^{-2} yr^{-1}) simulated by CLM4.0-FUN2.0.

root uptake dominates in the tropics and the subtropics of the northern hemisphere (excluding the deserts). In contrast, ECM root uptake of N dominates in high-latitude regions, especially in boreal forests (Fig. 3). At the global scale, AM-associated uptake is 562.2 Tg N yr^{-1} and 83% of the total mycorrhizal root uptake, while ECM-associated uptake is 111.4 Tg N yr^{-1} and 17% of the total mycorrhizal root uptake. Further, the magnitude of N uptake by each pathway mirrors the distribution of vegetation C (i.e., the total of structural and nonstructural vegetation carbon) in AM- and ECM-associated PFT's (82% and 18%, respectively).

Globally, symbiotic BNF comprises 69.0 Tg N yr^{-1}, nearly an order of magnitude less than the total of mycorrhizal and nonmycorrhizal root uptake. In the northern hemisphere, forest ecosystems have higher symbiotic BNF rates than other ecosystems (Fig. 2c).

The highest rates of symbiotic BNF are within 38°–34°S and 18°–15°S. In the northern hemisphere, this rate peaks at 6°–10°N. The 38°–52°N region has a high zonal symbiotic BNF amount, which is partly a function of greater land surface in this region.

Summing across the globe, the amount of N retranslocated from leaves is 177.5 Tg N yr^{-1}. Tropical forests and forested regions in the southeastern USA and China have the highest retranslocation rates (Fig. 2d). These are driven by high leaf area and the subsequent high leaf N simulated by CLM4.0–FUN2.0. Areas with low soil N like the low- and mid-latitude arid- and semiarid regions (i.e., the Sahel and the Tibet Plateau) also have high retranslocation rates (Fig. 2d). Areas with low leaf N like high-latitude regions covered by tundra ecosystems have the lowest retranslocation rates globally (Fig. 2d). There were also differences
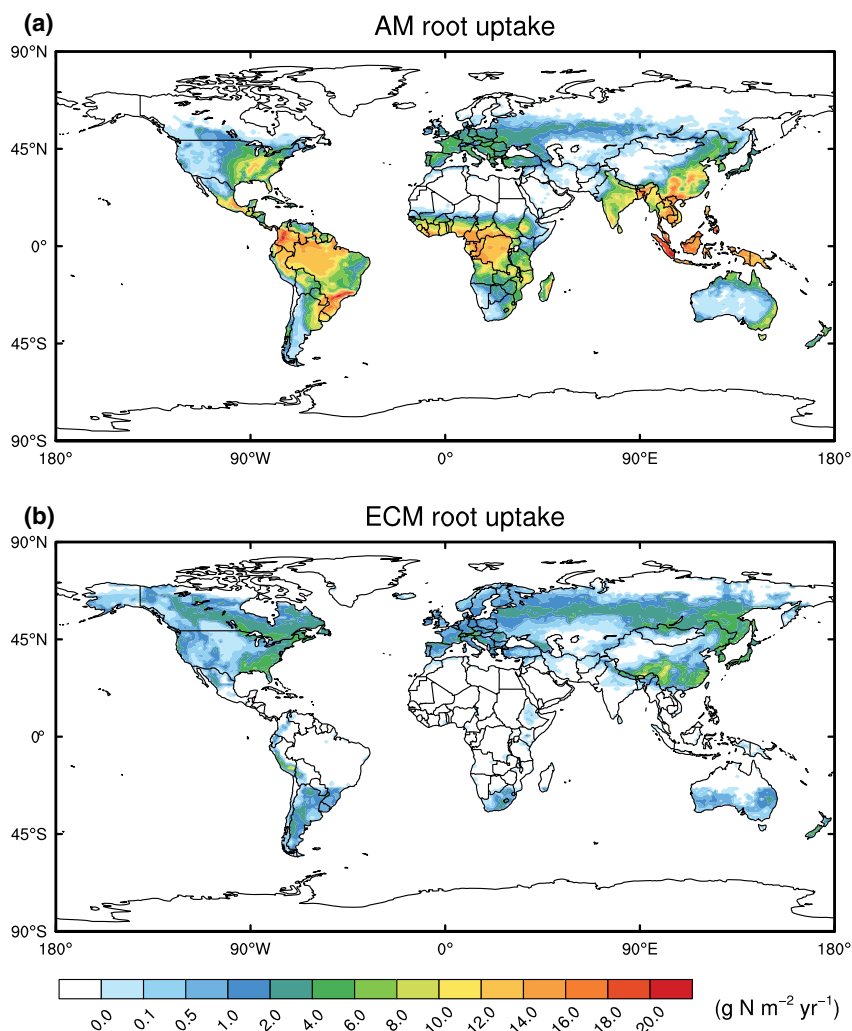

Fig. 3 The global mean annual (1995–2004) (a) arbuscular mycorrhizal (AM)-associated uptake and (b) ectomycorrhizal (ECM)-associated N uptake (g N m^{-2} yr^{-1}) simulated by CLM4.0-FUN2.0.

in the global distribution of retranslocation efficiency (i.e., the ratio of the retranslocated N to the amount of N in dead leaves prior to senescence) (Fig. 4). The retranslocation ratio ranges from 20% to 50% in tropical forests, from 40% to 70% in temperate forests, and from 20% to 70% in boreal forests. In the grassland and shrubland, the retranslocation ratio ranges from 1% in the tropics to 70% in the mid- and high-latitude regions. While the retranslocation ratio is originally set in CLM4.0 at constant 50% everywhere, the global spatially varying mean retranslocation ratio of CLM4.0–FUN2.0 is ~40%.

Zonal distributions show that mycorrhizal root uptake, which is dominated by AM roots in the tropics and subtropics, and by ECM roots in the high latitudes (Fig. 3), is the most important uptake pathway among the five uptake pathways globally (Fig. 5a, b). The AM root and ECM root uptake amounts are 55% and 11% of the global total N uptake, respectively. Mycorrhizal root uptake is 66% of the global total N uptake, and this value varies with the global distribution of the AM- and ECM-associated PFTs (Table 2) as a result of the different C cost for N acquisition between these two types of PFTs (Leake *et al.*, 2004; Phillips *et al.*, 2013; Soudzilovskaia *et al.*, 2015). Non-mycorrhizal root uptake has a similar zonal distribution to that of mycorrhizal root uptake (Fig. 5a, b) and is 10% of the global total N uptake. Retranslocated N is the second most important uptake pathway at 17% of the global total N uptake. Compared to the other N uptake pathways, the contribution of symbiotic BNF is minor, and it is only 7% of the global total N uptake. The fraction of symbiotic BNF increases toward the Poles (Fig. 5b). Passive N uptake has the

lowest contribution (Fig. 5b) and its amount peaks in 0°–3°S (Fig. 5a). Summing across all five pathways, N uptake peaks at 4°S, and the highest N uptake regions are in the tropics (Fig. 5a).

The seasonal pattern of N uptake varied across biomes (Fig. 6). In every biome, there was a significant amount of N demand that was not met through uptake. This was highest in grassland (477.7 Tg N yr^{-1}) and lowest in deciduous needleleaf forest (7.4 Tg N yr^{-1}) (Fig. 6). Both evergreen needleleaf forest and shrubland have the highest unmet N demand at 68%, and evergreen broadleaf forest has the smallest unmet N demand at 53%. For comparison, the global mean unmet N demand ratio simulated by CLM4.0 is 65%, while that of CLM4.0–FUN2.0 is 62%. The high unmet N demand ratios in different biomes are associated with the low soil N availability in CLM4.0. There was little seasonality in evergreen broadleaf forest (Fig. 6e). In deciduous broadleaf forest, deciduous needleleaf forest, and shrubland, which belong to either the seasonal-deciduous or stress-deciduous PFTs, there were two peaks in N demand and uptake that corresponded to the peaks of the growing season and senescence (Fig. 6a, d, f). Among the six biomes, evergreen broadleaf forest, which are the most biomass abundant PFTs, has the highest area-based retranslocation and total N uptake rates with values of 2.6 g N m^{-2} yr^{-1} and 17.1 g N m^{-2} yr^{-1}, respectively. Evergreen broadleaf forest also has the highest total N uptake rate at 273.4 Tg N yr^{-1}. In contrast, shrubland has the lowest area-based total N uptake rate with the value 1.9 g N m^{-2} yr^{-1}, and its retranslocation rate is the second lowest at 0.5 g N m^{-2} yr^{-1}. Deciduous needleleaf forest has the lowest total N uptake rate at 4.1 Tg N yr^{-1}.
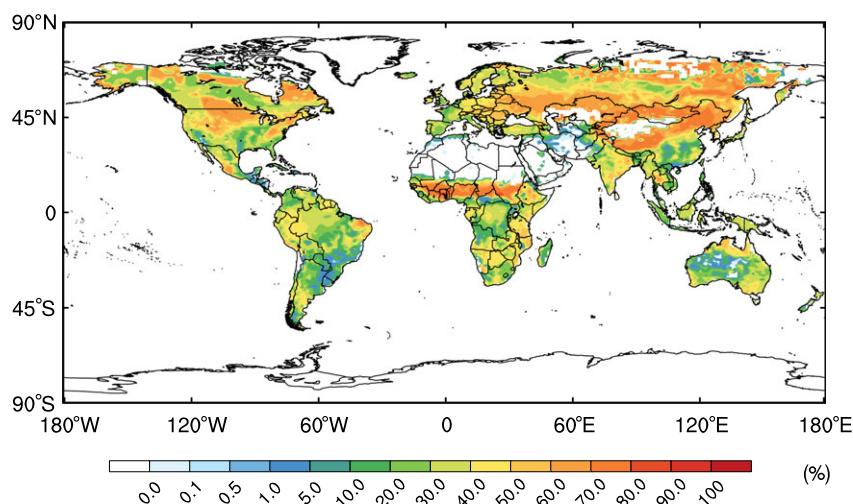

Fig. 4 The global mean annual (1995–2004) retranslocation ratio simulated by CLM4.0-FUN2.0.
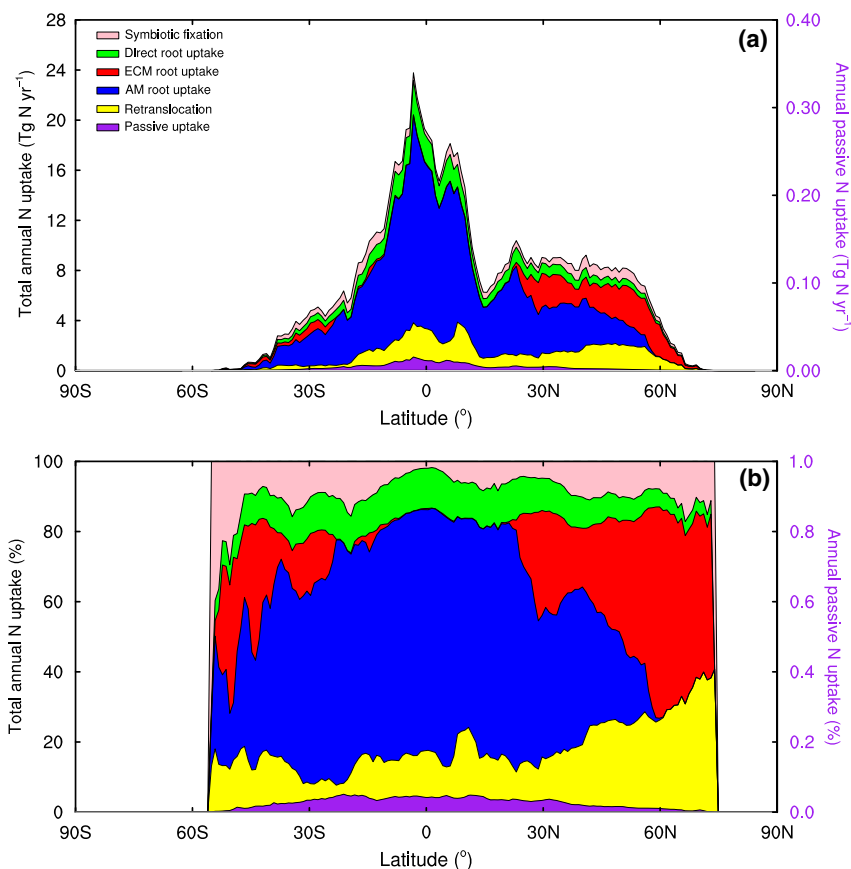
Fig. 5 The global mean annual (1995–2004) zonal distribution of the a) N uptake amount (Tg N yr^{-1}) and b) N uptake fraction simulated by CLM4.0-FUN2.0.

How does the C cost of N acquisition vary spatially and temporally?

CLM4.0–FUN2.0 estimated that 1.5% of GPP or 2.4 Pg C yr^{-1} is spent by plants to take up N. The greatest amount of C was spent on mycorrhizal root uptake of N, which is 1238.5 Tg C yr^{-1} and 52% of the global total used C (Fig. S4). The C amounts spent on retranslocation, symbiotic BNF, and nonmycorrhizal root uptake are 565.8, 399.3, and 199.0 Tg C yr^{-1}, respectively, which are 24%, 16%, and 8% of the total used C amount, respectively. The zonal regions with the highest C spent on N uptake are 7°–20°S, 9°–12°N, and 37°–53°N (Fig. S4). Examining dominant biomes shows that the vast majority of C spent on acquiring N is used to support mycorrhizal root uptake (Fig. 7). The deciduous broadleaf forest has the highest C use rate for N acquisition (25.9 ± 4.5 g C m^{-2} yr^{-1}) with 53% of the total C spent on N acquisition used to support mycorrhizal root uptake (Fig. 7). Grassland is similar with a nearly identical total magnitude as well as distribution of uptake across pathways. Evergreen broadleaf forest has 71% of the total C spent on N acquisition used to

support mycorrhizal root uptake, and this rate is the highest among the six ecosystems. However, evergreen broadleaf forest has the fifth total C use rate at 11.6 ± 2.3 g C m^{-2} yr^{-1} (Fig. 7).

Generally, the model simulated the highest relative costs of N uptake in high latitudes and the lowest in the tropics (Fig. 8). Here, we define the C use ratio as the ratio of the C spent on N acquisition to the total C available for allocation by the plant. Even with the highest total N uptake, tropical forest has the lowest C use ratio, which ranges from 0.1% to 1.0%. This distribution pattern is associated with the high N availability (Fig. S2) and high GPP per unit area in these regions (Figure not shown). The C use ratio varies from 0.5% to 4% in the boreal forest, southeast USA, and southeast China. In other systems, the ratio is much higher. In grasslands and croplands, including those in the Great Plains of the USA, Australia, and India, the C use ratio ranges from 2% to 20%. Finally, the ratio peaks in systems with low productivity including the arid- and semiarid regions and high-latitude shrublands, which have C use ratios that range from 8% to 80% (Fig. 8). Overall, tropical and boreal
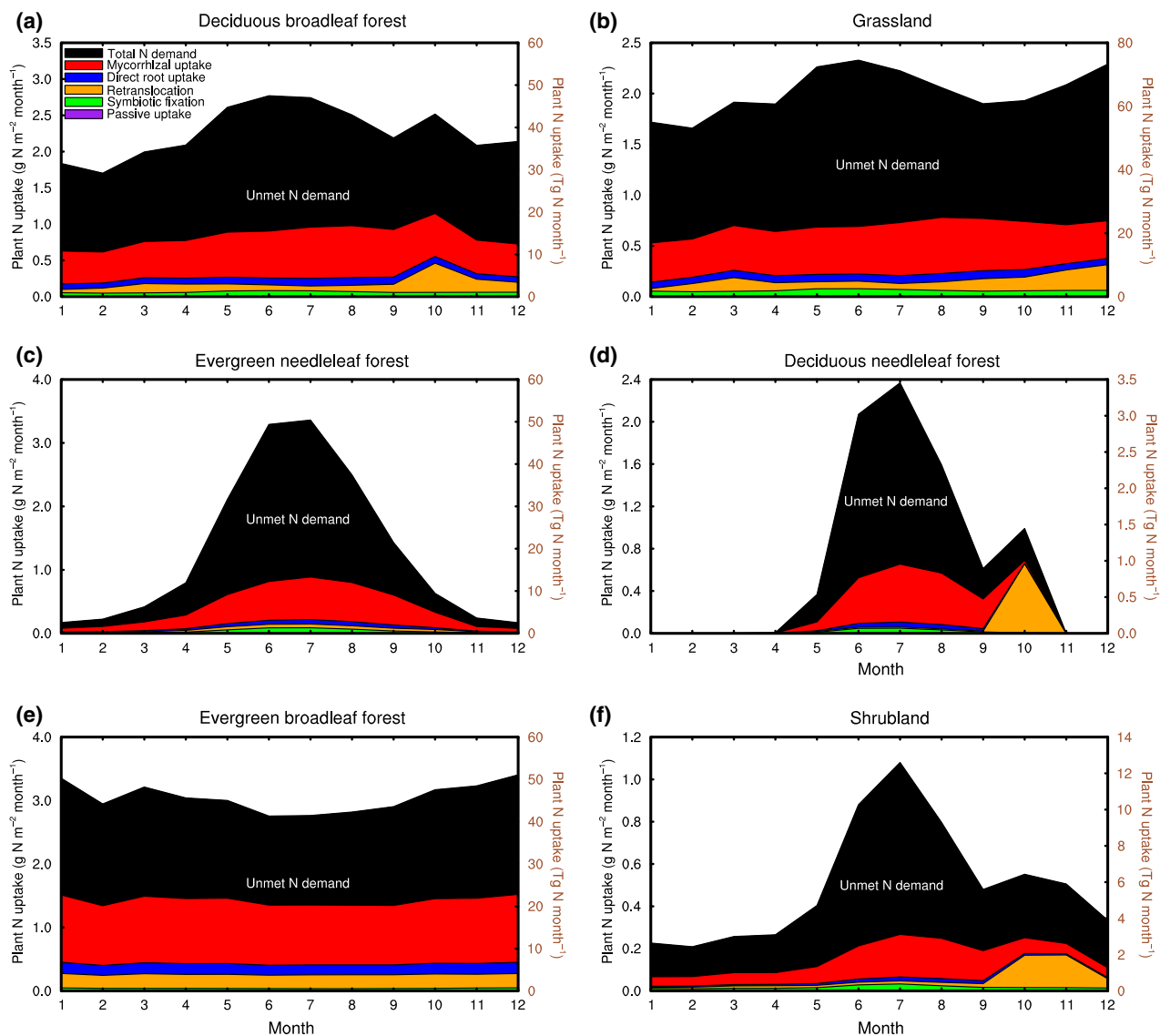
Fig. 6 The global mean monthly (1995–2004) N uptake simulated by CLM4.0-FUN2.0 in (a) deciduous broadleaf forest, (b) grassland, (c) evergreen needleleaf forest, (d) deciduous needleleaf forest, (e) evergreen broadleaf forest, and (f) shrubland.

forests have the lowest C costs on per unit area basis (Fig. S5).

How sensitive is the land C sink to a dynamic prediction of the C cost of N acquisition?

CLM4.0–FUN2.0 simulated that NPP was 50.8 Pg C yr^{-1}, which is 7.3 Pg C yr^{-1} less than that simulated by CLM4.0. This equates to a 13% reduction in global annual NPP. Zonally, NPP is reduced across all latitudes in CLM4.0–FUN2.0 relative to CLM4.0 (Fig. 9). On an absolute basis, the reduced NPP amount peaks at 2°S and decreases toward the Poles (Fig. 9). On a percentage basis, the reductions are greatest in

high-latitude regions and smallest in tropics (Fig. S6). Moreover, NPP decreases in all of the six most dominant biomes (Figs S7 and S8). Evergreen broadleaf forest has the largest NPP downregulation rates, which are 107.8 g C m^{-2} yr^{-1} and 1.7 Tg C yr^{-1}, while deciduous needleleaf forest has the smallest NPP downregulation rates, which are 8.3 g C m^{-2} yr^{-1} and 1.2 × 10^{-2} Tg C yr^{-1}. On a percentage basis, shrubland has the greatest downregulated NPP at 30% followed by grassland at 14%. Forests have smaller NPP downregulation ratios ranging from 6% in evergreen needleleaf forest to 11% in deciduous broadleaf forest. This variation reflects the high N-limitation in shrubland and grassland simulated by CLM4.0 (Thomas *et al.*, 2013).
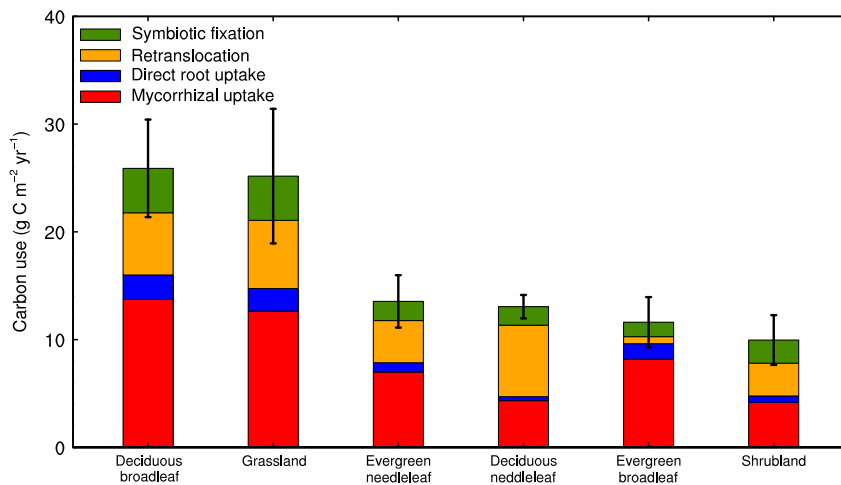
Fig. 7 The global mean annual (1995–2004) C used by N acquisition in deciduous broadleaf forest, grassland, evergreen needleleaf forest, deciduous needleleaf forest, evergreen broadleaf forest, and shrubland. Error bars are ±1 standard deviation.
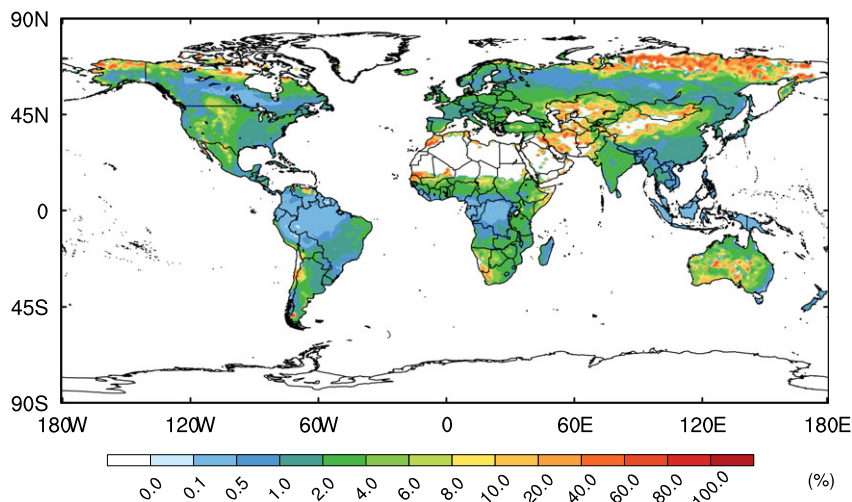

Fig. 8 The global mean annual (1995–2004) C use ratio simulated by CLM4.0-FUN2.0.

Discussion

This study shows the significant impacts of plant N dynamics on global C cycling, and the coupled model gives a new approach for improving terrestrial C sinks associated with N-limitation in TBMs, which is crucial to climate models and Earth system models. In addition, the partition of C transfers between free-living microbes, mycorrhizal fungi, and symbiotic N-fixing fungi at the global scale has important implications, particularly for the next-generation soil C models that model the impacts of these C transfers but often assume that they are a fixed percentage of NPP (Wieder *et al.*, 2013; Sulman *et al.*, 2014).

Much of the uncertainty in TBM predictions of the future land C sink is driven by how TBMs prescribe nutrient constraints on primary production (Fisher *et al.*, 2012; Fernández-Martínez *et al.*, 2014).Using a cutting edge plant N model (i.e., FUN2.0) coupled into CLM4.0, this research addressed this uncertainty by dynamically predicting the C cost of N acquisition. Specifically, we evaluated the amounts, spatial distributions, and seasonality of N acquisition; the amounts and spatial distributions of C used for N acquisition; and NPP variations as a result of N acquisition and allocation at the global scale. CLM4.0–FUN2.0 is able to reproduce reasonable global N uptake and C use distributions that provide an important dynamic constraint on predictions of the future land C sink.

Overall, the global total N uptake is 1.0 Pg N yr^{-1}, and the mycorrhizal root uptake is the dominant N uptake pathway. Mycorrhizal root uptake is the largest
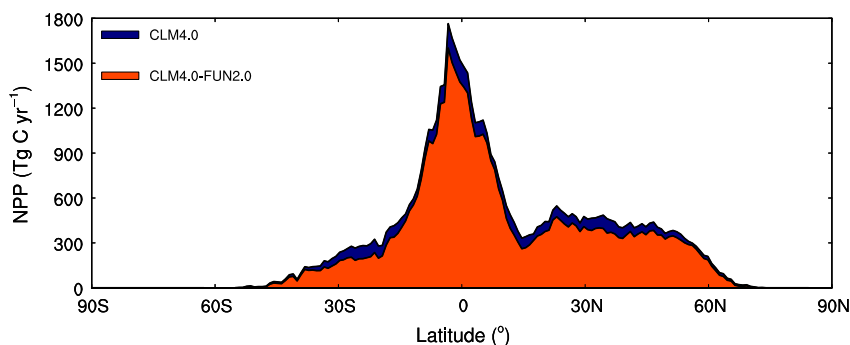
Fig. 9 The mean annual (1995–2004) zonal NPP (Tg C yr^{-1}) simulated by CLM4.0 and CLM4.0-FUN2.0.

C cost followed by retranslocation, symbiotic BNF, and nonmycorrhizal root uptake. The total C use of these four N uptake pathways is 2.4 Pg C yr^{-1}; this C is respired by plant (i.e., C used for retranslocation) and soil (i.e., C used for mycorrhizal root and nonmycorrhizal root uptake and symbiotic BNF), and added to autotrophic respiration and soil heterotrophic respiration, respectively. The total C use is 1.5% of global GPP. Compared to the FLUXNET model tree ensembles (global GPP is 117 Pg C yr^{-1}) and other TBM simulations (e.g., CLM version 4.5; global GPP is 130 Pg C yr^{-1}) (Beer *et al.*, 2010; Bonan *et al.*, 2011; Jung *et al.*, 2011), CLM4.0 overestimates global GPP (particularly in the tropics). Coupling FUN2.0 to CLM4.0 helped to reduce the high bias by 5%, but the resultant GPP is still biased high. The high-biased GPP also results in a high leaf area index (LAI) bias (e.g., as compared to the Moderate Resolution Imaging Spectroradiometer (MODIS) observed LAI). CLM4.0–FUN2.0 reduced the high LAI bias by 18% globally and 20% in the tropics. The amount of available C for N acquisition from CLM4.0–FUN2.0 is higher than that predicted in other models, and this may result in biased simulations of N acquisition and C cost. Reduction of available C in CLM4.5 would reduce that bias. The CLM4.0–FUN2.0-simulated NPP is 50.8 Pg C yr^{-1}, which is 7.3 Pg C yr^{-1} (i.e., 13%) less than that of CLM4.0.

Biome-level variation

N acquisition and C use varied among biomes. In general, forest ecosystems had greater mycorrhizal root uptake rates than other ecosystems (Fig. 2). The AM-associated and ECM-associated N uptake pattern is generally consistent with the AM- and ECM-plant distribution discussed in Read (1991). The ecosystems north of 30°N have higher retranslocation fractions than other ecosystems (Fig. 5b), which is related to the increase of N-limitation in these regions (Wang *et al.*, 2010). The global symbiotic BNF pattern predicted by

CLM4.0–FUN2.0 is similar to an empirical estimate by Cleveland *et al.* (2013). However, our modeling work provides an important estimate of the global cost of BNF at 399.3 Tg C yr^{-1}. Evergreen broadleaf forest, which is the most productive biome (i.e., with the highest area-based NPP value; Fig. S7), has the highest N uptake rate and lowest unmet N demand ratio among the six biomes. On the contrary, shrubland has the lowest area-based NPP value, and it has the lowest N uptake rate and the highest unmet N demand ratio. As the area-based GPP values have a similar partition pattern to that of the NPP values among the six biomes (figure not shown), the results demonstrate ecosystem productivity is a crucial driver for N uptake suggesting that plants can upregulate their C investment to gain N. Globally, N acquisition uses 2.4 Pg C yr^{-1}. Deciduous broadleaf forest, which has the second highest area-based N uptake rate and NPP value, has the highest area-based C use rate of N acquisition. This result shows that the C cost of N acquisition is a function of both ecosystem productivity and environmental conditions (i.e., soil N and temperature). Specifically, soil temperature directly affects the cost of symbiotic BNF and indirectly affects the cost of mycorrhizal and non-mycorrhizal root uptake and retranslocation by changing the ecosystem carbon stocks and decomposition rates. Tropical forests have the lowest C use ratio among all the ecosystems (Fig. 8), which likely reflects P-limitation rather than N-limitation in the tropics (Wang *et al.*, 2010). The C use ratio increases with latitude reflecting decreasing N availability with latitude moving from temperate forests to boreal forests to tundra ecosystems. This decrease in available N reflects temperature constraints on C and N mineralization in the model.

Symbiotic BNF evaluation

CLM4.0–FUN2.0 estimates of symbiotic BNF are well within the error of recent empirical estimates of global

fixation rates. Our estimate of global symbiotic BNF is 69.0 Tg N yr^{-1}, which is 9% of the total of mycorrhizal and nonmycorrhizal root uptake. Cleveland *et al.* (2013) suggested that recycled N accounts for nearly 90% of annual terrestrial plant demand; therefore, the contribution of different N uptake pathways is reasonably simulated by CLM4.0–FUN2.0. The symbiotic BNF estimations discussed in this study rely on CLM's framework for predicting total fixation and use FUN to predict the fraction that is driven by symbiotic microbes. CLM4.0–FUN2.0 predicts that total fixation is 110.4 Tg N yr^{-1} with 63% (i.e., 69.0 Tg N yr^{-1}) of this driven by symbiotic N-fixers. Recent global empirical estimates suggest that the global total BNF is 127.5 Tg N yr^{-1}, of which 82% is symbiotic (105.1 Tg N yr^{-1}) (Cleveland *et al.*, 2013). On a per unit area basis, CLM4.0–FUN2.0 predicted 0.78 g N m^{-2} yr^{-1}, whereas empirical estimates are around 0.85 g N m^{-2} yr^{-1} (Sullivan *et al.*, 2014). This agreement is remarkably similar given that our estimates are derived from a mechanistic full N cycle in a complex TBM, and their estimates are derived from upscaling of extensive field measurements. Spatially, the CLM4.0–FUN2.0-simulated global symbiotic BNF pattern is similar to empirical estimates as well, which indicate a lower tropical forest symbiotic BNF due to the internal pools of bioavailable N these systems build (Hedin *et al.*, 2009; Sullivan *et al.*, 2014). However, the symbiotic BNF rate simulated by CLM4.0–FUN2.0 is lower than that discussed in Cleveland *et al.* (2013), which is likely driven by the cost (i.e., economic) structure of FUN and the differences of soil temperature and N$_2$ fixing ability of roots between CLM4.0–FUN2.0 and that from Cleveland *et al.* (2013).

Benchmarking CLM4.0–FUN2.0

Benchmarking global model products is a challenge for the entire TBM (Luo *et al.*, 2012; Kelley *et al.*, 2013; Schwalm *et al.*, 2013). To validate the broadscale patterns in the C cost of N acquisition, we leveraged a new global nutrient limitation product developed from remote sensing (Fisher *et al.*, 2012). This product couples remotely sensed estimates of primary production and evapotranspiration to identify areas where light and water are not limiting productivity. In this benchmarking exercise, we expected the degree of NPP downregulation fraction predicted by CLM4.0–FUN2.0 would be correlated with the remotely sensed nutrient limitation product. Overall, the NPP downregulation fraction simulated by CLM4.0–FUN2.0 has the similar global distribution pattern to that of the nutrient limitation product. There was a bias with CLM4.0–FUN2.0 over-predicting NPP downregulation in low productivity systems including arid and semiarid regions and the tundra

region and under-predicting in high productivity systems, especially forest ecosystems (Fig. S9). However, this likely reflects the fact that the remotely sensed product captures other forms of nutrient limitation including P, especially with respect to our underestimation of downregulation the tropics. In particular, systems that are known to be more N-limited had higher correlations (e.g., nonarctic grassland; Fig. S10a) than systems known to be highly limited by P or other nutrients (e.g., broadleaf evergreen tropical forests; Fig. S10b) (Wang *et al.*, 2010; Thomas *et al.*, 2013). Nevertheless, the agreement between the two products highlights the robustness of the CLM4.0–FUN2.0 predictions with the remaining residual error emphasizing the need to incorporate P dynamics into FUN2.0 and CLM4.0–FUN2.0.

Emergent constraints from CLM4.0–FUN2.0

Although FUN2.0 focuses on plant-centric dynamics, the C transferred to the soil for N acquisition as well as the N inputs in fresh litter has important downstream impacts on predictions of soil C dynamics. In CLM4.0, soil respiration consists of heterotrophic respiration and root respiration. In CLM4.0–FUN2.0, by contrast, the C spent on soil N acquisition downregulates NPP, and this expended C is added to the heterotrophic respiration. Compared to CLM4.0, a 25-year CLM4.0–FUN2.0 simulation shows a pulse in heterotrophic respiration during the first two simulation years because of the new C source to heterotrophic respiration from FUN, but over time heterotrophic respiration declines relative to CLM4.0 because of reduced litter inputs into soil from N-limitation and subsequent NPP downregulation (Fig. 10). In CLM4.0–FUN2.0, the increased heterotrophic respiration amount is not equal to the reduced NPP amount as the C spent on leaf N resorption downregulates autotrophic respiration and N allocation change of the coupled model also regulates NPP variation trends. We chose to mass balance the C budget in this manner; however, this method wastes the C used for N acquisition as respiration and needs further improvement. It has been estimated that the total carbon flux to mycorrhizal fungi potentially contributes up to 30% of NPP in forest ecosystems (Courty *et al.*, 2010; Vicca *et al.*, 2012). Therefore, the ability of FUN to predict the C transfers by plants will have important implications in TBMs that include microbial function and priming (Wieder *et al.*, 2013; Sulman *et al.*, 2014). For example, once fully coupled with a soil-microbial model, FUN2.0 will predict the amount of C transferred into the labile soil C pool and the microbial model will predict the

impacts on SOM decomposition (i.e., both C and N mineralization). Thus, CLM4.0–FUN2.0 represents an important bridge between plant models and rapidly evolving soil-microbial models.

The C–N trade-off process has significant implications on climate models and Earth system models, particularly in assessing potential futures to Earth's climate. This study was developed initially for the offline CLM4.0 and CLM4.0–FUN2.0, which can be used as the land model of CESM, but current work is incorporating FUN2.0 into the next release version of CLM as well as integration into the fully coupled CESM. Generally, C–N dynamics constrain the terrestrial biosphere response to increasing atmospheric CO_2 concentration (Thornton *et al.*, 2007). With C–N cycle coupling in a global-coupled climate system model, Thornton *et al.* (2007) suggested that there would be reduced global terrestrial C uptake with increasing atmospheric CO_2. Zaehle *et al.* (2010) also reported reduced terrestrial C storage due to CO_2 fertilization within a climate model with surface C–N processes. Compared to CLM4.0, CLM4.0–FUN2.0 results in more ecosystem respiration and global terrestrial C uptake reduction, which implies accelerated atmospheric C accumulation and higher rates of climate change if it is coupled into CESM. This conclusion is in contrary to the results derived from LPJ-GUESS with C–N interactions implemented (Smith *et al.*, 2014; Wårlind *et al.*, 2014). This difference is assumed to be associated with the individual- and patch-based representations of vegetation structural dynamics represented by LPJ-GUESS (Smith *et al.*, 2014; Wårlind *et al.*, 2014). All these results suggest the uncertainty of present and future fate of biospheric C sinks associated with N-limitation. Besides the impacts on global C dynamics, CLM4.0–FUN2.0 also alters global N dynamics. Unlike the fixed retranslocation amount in CLM4.0, the new model also includes dynamically varying retranslocation. Compared to CLM4.0, CLM4.0–FUN2.0 simulates less soil

and retranslocated N uptake, which results in the increase of soil and total ecosystem N (figure not shown). This variation temporally reduces N-limitation, which can potentially lead to transient increases in C uptake during CO_2 fertilization (Wårlind *et al.*, 2014) in global climate models.

Soil N deficiency of CLM4.0

In many ecosystems, CLM4.0–FUN2.0 predicted that there was not enough soil N uptake to meet N_{demand} with the global average met N demand being 34% met. One reason for this is that CLM4.0 is known to underestimate the production of mineral N resulting in a highly N-limited terrestrial C sink (Koven *et al.*, 2013). Thus, the soil mineral N uptake simulated by CLM4.0–FUN2.0 is underestimated and much lower than the N demand (Fig. 6). To test mechanistically whether greater soil N availability would allow CLM4.0–FUN2.0 to predict uptake rates that meet demand, we ran an offline sensitivity test at a temperate forest site in southern Indiana, USA (Morgan Monroe State Forest AmeriFlux site). The N mineralization rate predicted by CLM4.0 is nearly half of the empirical estimates at the site (12 g N m^{-2} yr^{-1}; Ehman *et al.*, 2002). When we doubled soil mineral N, the CLM4.0–FUN2.0-simulated total soil N uptake increases from 5.5 g N m^{-2} yr^{-1}, which was 70% of N_{demand}, to 6.9 g N m^{-2} yr^{-1} and was within 99% of meeting demand (Fig. S11). Ongoing coupling of FUN2.0 into CLM4.5 and CLM5.0 (prerelease), which is the most recent version of CLM and includes a vertically resolved soil biogeochemistry scheme and a more realistic treatment of soil mineral N pools (Koven *et al.*, 2013), may lead to further improvements as these versions predict more soil N availability than CLM4.0. However, N mineralization rates will likely to be increased once model structures evolve to allow FUN to transfer C to the soil that primes SOM decomposition.
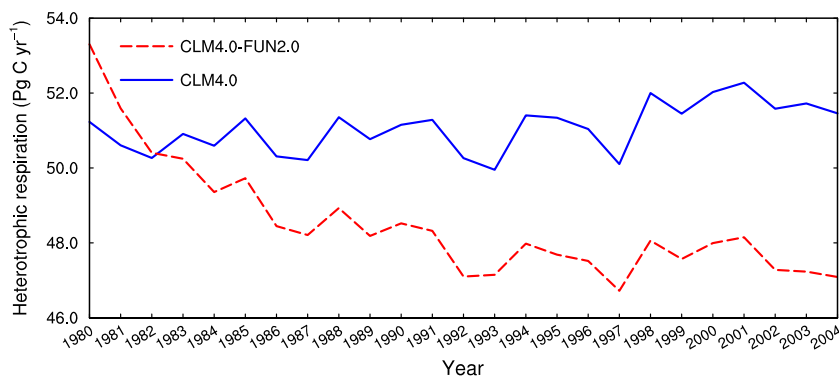

Fig. 10 The global annual total (1980–2004) heterotrophic respiration (Pg C yr^{-1}) simulated by CLM4.0 and CLM4.0-FUN2.0.

Further improvements to CLM4.0–FUN2.0

The nonstructural N pools in CLM4.0 need to be improved in the future. Generally, nonstructural carbohydrates, which are represented as the storage pools in TBMs, accumulate throughout the plant including leaves, stems, and roots (Millard & Grelet, 2010). Both retranslocated N and root N uptake can be used to augment N storage. Seasonal remobilization uses N from the storage pools by translocating N to other tissues for growth (Millard & Proe, 1991; Millard & Grelet, 2010). CLM4.0 includes vegetation C and N storage pools for leaves, stems, and roots, and the storage pools and the display pools are connected with the transfer pools. However, the retranslocated N pool is separated from the leaf N storage pool, and these two pools have different seasonality (Fig. S12). Compared to the leaf N storage pool, which has an onset-period decreasing trend, the retranslocated N pool has an offset-period decreasing trend at the Morgan Monroe site (Fig. S12a, b).

To better describe the season cycle of the nonstructural N and obtain the dynamic simulation of remobilization, we suggest combining the leaf N storage pool and the retranslocated N pool in CLM4.0. In deciduous forest, for example, the leaf N storage pool, which declines rapidly as soon as the growing season starts, is used as remobilization. The leaf N storage pool starts rising in the late growing season as a result of the slow growth and replenished nonstructural N pools (Dietze *et al.*, 2014). During the senescence period, the N storage pool would have another quick growth, which is associated with leaf N retranslocation. During the dormant season, the leaf N storage pool would decrease slowly to meet respiratory demand. This cycle can be applied to most seasonal-deciduous species (Dietze *et al.*, 2014) (Fig. S13) and the nonstructural pools of other phenological types can be similarly improved. Compared to the original CLM4.0, the new leaf N storage pool is more realistic and can potentially improve the N dynamics of CLM4.0.

Integrating P constraints to C uptake represents the next challenge for TBMs. Soil P dynamics, which limits C uptake at low latitudes, have been included in the biogeochemistry process module (i.e., Carnegie-Ames-Stanford Approach with C, N, and P cycles or CASA-CNP) of the Community Atmosphere Biosphere Land Exchange (CABLE) model (Wang *et al.*, 2010, 2011) as well as in CLM-CNP (Yang *et al.*, 2014). CABLE estimated that NPP was reduced by 20% on average as a result of P-limitation in tropical ecosystems (i.e., tropical evergreen broadleaf forests and tropical savannahs) (Wang *et al.*, 2010). Considering C–nutrient (i.e., N and P) interaction reduces both the benefits of reforestation and the cost of deforestation as indicated by the global terrestrial carbon balance (Wang, *et al.*, 2015). The research presented here does not model the C cost of P acquisition. However, the integration of P dynamics into CLM-CNP and continued development of global P data products are now making it feasible to add P uptake strategies into the cost structure of FUN. Given the modular structure of FUN, dynamic costs of P acquisition can easily be added to the resistance network. Thus, FUN is well poised for meeting the challenge of including plant P dynamics into the next generation of TBMs.

Acknowledgements

References

Allen EB, Allen MF, Helm DJ, Trappe JM, Molina R, Rincon E (1995) Patterns and regulation of mycorrhizal plant and fungal diversity. *Plant and Soil*, **170**, 47–62.

Beer C, Reichstein M, Tomelleri E *et al.* (2010) Terrestrial gross carbon dioxide uptake: global distribution and covariation with climate. *Science*, **329**, 834–838.

Bloom AJ, Chapin FS, Mooney HA (1985) Resource limitation in plants – an economic analogy. *Annual Review of Ecology and Systematics*, **16**, 363–392.

Bonan GB, Levis S (2006) Evaluating aspects of the Community Land and Atmosphere Models (CLM3 and CAM3) using a dynamic global vegetation model. *Journal of Climate*, **19**, 2290–2301.

Bonan GB, Lawrence PJ, Oleson KW *et al.* (2011) Improving canopy processes in the Community Land Model version 4 (CLM4) using global flux fields empirically inferred from FLUXNET data. *Journal of Geophysical Research: Biogeosciences*, **116**, G02014.

Brzostek ER, Fisher JB, Phillips RP (2014) Modeling the carbon cost of plant nitrogen acquisition: mycorrhizal trade-offs and multipath resistance uptake improve predictions of retranslocation. *Journal of Geophysical Research: Biogeosciences*, **119**, 1684–1697.

Brzostek ER, Dragoni D, Brown ZA, Phillips RP (2015) Mycorrhizal type determines the magnitude and direction of root-induced changes in decomposition in a temperate forest. *New Phytologist*, **206**, 1274–1282.

Cai X, Yang Z-L, Fisher JB, Zhang X, Barlage M, Chen F (2015) Integration of nitrogen dynamics into the Noah-MP land surface model for climate and environmental predictions. Submitted to Geoscientific Model Development Discussion, **8**, 4113–4153.

Cleveland CC, Houlton BZ, Smith WK *et al.* (2013) Patterns of new versus recycled primary production in the terrestrial biosphere. *Proceedings of the National Academy of Sciences of the United States of America*, **110**, 12733–12737.

Courty P-E, Buée M, Diedhiou AG *et al.* (2010) The role of ectomycorrhizal communities in forest ecosystem processes: new perspectives and emerging concepts. *Soil Biology and Biochemistry*, **42**, 679–698.

Dickinson RE, Berry JA, Bonan GB *et al.* (2002) Nitrogen controls on climate model evapotranspiration. *Journal of Climate*, **15**, 278–295.

Dickinson RE, Oleson KW, Bonan GB *et al.* (2006) The Community Land Model and its climate statistics as a component of the Community Climate System Model. *Journal of Climate*, **19**, 2302–2324.

Dietze MC, Sala A, Carbone MS, Czimczik CI, Mantooth JA, Richardson AD, Vargas R (2014) Nonstructural carbon in woody plants. *Annual Review of Plant Biology*, **65**, 667–687.

Duchesne L, Ouimet R, Camiré C, Houle D (2001) Seasonal nutrient transfers by foliar resorption, leaching, and litter fall in a northern hardwood forest at Lake Clair Watershed, Quebec, Canada. *Canadian Journal of Forest Research*, **31**, 333–344.

Ehman JL, Schmid HP, Grimmond CSB, Randolph JC, Hanson PJ, Wayson CA, Cropley FD (2002) An initial intercomparison of micrometeorological and ecological inventory estimates of carbon exchange in a mid-latitude deciduous forest. *Global Change Biology*, **8**, 575–589.

Falkengren-Grerup U (1995) Interspecies differences in the preference of ammonium and nitrate in vascular plants. *Oecologia*, **102**, 305–311.

Fernández-Martínez M, Vicca S, Janssens IA *et al.* (2014) Nutrient availability as the key regulator of global forest carbon balance. *Nature Climate Change*, **4**, 471–476.

Fisher JB, Sitch S, Malhi Y, Fisher RA, Huntingford C, Tan S-Y (2010) Carbon cost of plant nitrogen acquisition: a mechanistic, globally applicable model of plant nitrogen uptake, retranslocation, and fixation. *Global Biogeochemical Cycles*, **24**, GB1014.

Fisher JB, Badgley G, Blyth E (2012) Global nutrient limitation in terrestrial vegetation. *Global Biogeochemical Cycles*, **26**, GB3007.

Fisher JB, Huntzinger DN, Schwalm CR, Sitch S (2014) Modeling the terrestrial biosphere. *Annual Review of Environment and Resources*, **39**, 91–123.

Gent PR, Danabasoglu G, Donner LJ *et al.* (2011) The community climate system model version 4. *Journal of Climate*, **24**, 4973–4991.

Hedin LO, Brookshire ENJ, Menge DNL, Barron AR (2009) The nitrogen paradox in tropical forest ecosystems. *Annual Review of Ecology, Evolution, and Systematics*, **40**, 613–635.

Hobbie EA (2006) Carbon allocation to ectomycorrhizal fungi correlates with belowground allocation in culture studies. *Ecology*, **87**, 563–569.

Högberg MN, Högberg P (2002) Extramatrical ectomycorrhizal mycelium contributes one-third of microbial biomass and produces, together with associated roots, half the dissolved organic carbon in a forest soil. *New Phytologist*, **154**, 791–795.

Holopainen JK, Peltonen P (2002) Bright autumn colours of deciduous trees attract aphids: nutrient retranslocation hypothesis. *Oikos*, **99**, 184–188.

Houlton BZ, Wang Y-P, Vitousek PM, Field CB (2008) A unifying framework for dinitrogen fixation in the terrestrial biosphere. *Nature*, **454**, 327–330.

Huntzinger DN, Schwalm C, Michalak AM *et al.* (2013) The North American carbon program multi-scale synthesis and terrestrial model intercomparison project – part 1: overview and experimental design. *Geoscientific Model Development*, **6**, 2121–2133.

Jones DL, Healey JR, Willett VB, Farrar JF, Hodge A (2005) Dissolved organic nitrogen uptake by plants – an important N uptake pathway? *Soil Biology and Biochemistry*, **37**, 413–423.

Jung M, Reichstein M, Margolis HA *et al.* (2011) Global patterns of land-atmosphere fluxes of carbon dioxide, latent heat, and sensible heat derived from eddy covariance, satellite, and meteorological observations. *Journal of Geophysical Research: Biogeosciences*, **116**, G00J07.

Kelley DI, Prentice IC, Harrison SP, Wang H, Simard M, Fisher JB, Willis KO (2013) A comprehensive benchmarking system for evaluating global vegetation models. *Biogeosciences*, **10**, 3313–3340.

Koven CD, Riley WJ, Subin ZM *et al.* (2013) The effect of vertically resolved soil biogeochemistry and alternate soil C and N models on C dynamics of CLM4. *Biogeosciences*, **10**, 7109–7131.

Lamarque J-F, Dentener F, Mcconnell J *et al.* (2013) Multi-model mean nitrogen and sulfur deposition from the Atmospheric Chemistry and Climate Model Intercomparison Project (ACCMIP): evaluation of historical and projected future changes. *Atmospheric Chemistry and Physics*, **13**, 7997–8018.

Lawrence DM, Oleson KW, Flanner MG *et al.* (2011) Parameterization improvements and functional and structural advances in Version 4 of the Community Land Model. *Journal of Advances in Modeling Earth Systems*, **3**, M03001.

Leake J, Johnson D, Donnelly D, Muckle G, Boddy L, Read D (2004) Networks of power and influence: the role of mycorrhizal mycelium in controlling plant communities and agroecosystem functioning. *Canadian Journal of Botany*, **82**, 1016–1045.

Lebauer DS, Treseder KK (2008) Nitrogen limitation of net primary productivity in terrestrial ecosystems is globally distributed. *Ecology*, **89**, 371–379.

Luo YQ, Randerson JT, Abramowitz G *et al.* (2012) A framework for benchmarking land models. *Biogeosciences*, **9**, 1899–1944.

Marschner H (1995) *Mineral Nutrition of Higher Plants*, 2nd edn. Academic, New York. ISBN 978-0-12-473542-2.

Millard P, Grelet GA (2010) Nitrogen storage and remobilization by trees: ecophysiological relevance in a changing world. *Tree Physiology*, **30**, 1083–1095.

Millard P, Proe MF (1991) Leaf demography and the seasonal internal cycling of nitrogen in sycamore (*Acer pseudoplatanus* L.) seedlings in relation to nitrogen supply. *New Phytologist*, **117**, 587–596.

Nordin A, Högberg P, Näsholm T (2001) Soil nitrogen form and plant nitrogen uptake along a boreal forest productivity gradient. *Oecologia*, **129**, 125–132.

Oleson KW, Dai Y, Bonan GB *et al.* (2004) Technical description of the Community Land Model (CLM). NCAR Technical Note, NCAR/TN-461 + STR, National Center for Atmospheric Research, Boulder, CO.

Oleson KW, Lawrence DM, Bonan GB *et al.* (2010) Technical description of version 4.0 of the Community Land Model. NCAR Technical Note, NCAR/TN-478 + STR, National Center for Atmospheric Research, Boulder, CO.

Ostle NJ, Smith P, Fisher RA *et al.* (2009) Integrating plant–soil interactions into global carbon cycle models. *Journal of Ecology*, **97**, 851–863.

Phillips RP, Brzostek ER, Midgley MG (2013) The mycorrhizal-associated nutrient economy: a new framework for predicting carbon–nutrient couplings in temperate forests. *New Phytologist*, **199**, 41–51.

Qian T, Dai A, Trenberth KW, Oleson KW (2006) Simulation of global land surface conditions from 1948 to 2004. part I: forcing data and evaluations. *Journal of Hydrometeorology*, **7**, 953–975.

Rastetter EB, Ågren GI, Shaver GR (1997) Responses of N-limited ecosystems to increased CO_2: a balanced-nutrition, coupled-element-cycles model. *Ecological Applications*, **7**, 444–460.

Rastetter EB, Vitousek PM, Field C, Shaver GR, Herbert D, Ågren GI (2001) Resource optimization and symbiotic nitrogen fixation. *Ecosystems*, **4**, 369–388.

Read DJ (1991) Mycorrhizas in ecosystems. *Experientia*, **47**, 376–391.

Schwalm CR, Huntinzger DN, Michalak AM *et al.* (2013) Sensitivity of inferred climate model skill to evaluation decisions: a case study using CMIP5 evapotranspiration. *Environmental Research Letters*, **8**, 024028.

Shi M, Yang Z-L, Lawrence DM, Dickinson RE, Subin ZM (2013) Spin-up processes in the Community Land Model Version 4 with explicit carbon and nitrogen components. *Ecological Modelling*, **263**, 308–325.

Smith B, Wårlind D, Arneth A, Hickler T, Leadley P, Siltberg J, Zaehle S (2014) Implications of incorporating N cycling and N limitations on primary production in an individual-based dynamic vegetation model. *Biogeosciences*, **11**, 2027–2054.

Soudzilovskaia NA, van der Heijden MGA, Cornelissen JHC *et al.* (2015) Quantitative assessment of the differential impacts of arbuscular and ectomycorrhiza on soil carbon cycling. *New Phytologist*, **208**, 280–293.

Sullivan BW, Smith WK, Townsend AR, Nasto MK, Reed SC, Chazdon RL, Cleveland CC (2014) Spatially robust estimates of biological nitrogen (N) fixation imply substantial human alteration of the tropical N cycle. *Proceedings of the National Academy of Sciences of the United States of America*, **111**, 8101–8106.

Sulman BN, Phillips RP, Oishi AC, Shevliakova E, Pacala SW (2014) Microbe-driven turnover offsets mineral-mediated storage of soil carbon under elevated CO_2. *Nature Climate Change*, **4**, 1099–1102.

Thomas RQ, Zaehle S, Templer PH, Goodale CL (2013) Global patterns of nitrogen limitation: confronting two global biogeochemical models with observations. *Global Change Biology*, **19**, 2986–2998.

Thornton PE, Rosenbloom NA (2005) Ecosystem model spin-up: estimating steady state conditions in a coupled terrestrial carbon and nitrogen cycle model. *Ecological Modelling*, **189**, 25–48.

Thornton PE, Zimmermann NE (2007) An improved canopy integration scheme for a land surface model with prognostic canopy structure. *Journal of Climate*, **20**, 3902–3923.

Thornton PE, Law BE, Gholz HL *et al.* (2002) Modeling and measuring the effects of disturbance history and climate on carbon and water budgets in evergreen needleleaf forests. *Agricultural and Forest Meteorology*, **113**, 185–222.

Thornton PE, Lamarque J-F, Rosenbloom NA, Mahowald NM (2007) Influence of carbon-nitrogen cycle coupling on land model response to CO_2 fertilization and climate variability. *Global Biogeochemical Cycles*, **21**, GB4018.

Thornton PE, Doney SC, Lindsay K *et al.* (2009) Carbon-nitrogen interactions regulate climate-carbon cycle feedbacks: results from an atmosphere-ocean general circulation model. *Biogeosciences*, **6**, 2099–2120.

Vicca S, Luyssaert S, Penuelas J *et al.* (2012) Fertile forests produce biomass more efficiently. *Ecology Letters*, **15**, 520–526.

Vitousek PM, Field CB (1999) Ecosystem constraints to symbiotic nitrogen fixers: a simple model and its implications. *Biogeochemistry*, **46**, 179–202.

Vitousek PM, Howarth RW (1991) Nitrogen limitation on land and in the sea: how can it occur? *Biogeochemistry*, **13**, 87–115.

Vitousek PM, Cassman K, Cleveland CC *et al.* (2002) Towards an ecological understanding of biological nitrogen fixation. *Biogeochemistry*, **57** (58), 1–45.

Wang Y-P, Houlton BZ, Field CB (2007) A model of biogeochemical cycles of carbon, nitrogen, and phosphorus including symbiotic nitrogen fixation and phosphatase production. *Global Biogeochemical Cycles*, **21**, GB1018.

Wang Y-P, Law RM, Pak B (2010) A global model of carbon, nitrogen and phosphorus cycles for the terrestrial biosphere. *Biogeosciences*, **7**, 2261–2282.

Wang Y-P, Kowalczyk E, Leuning R *et al.* (2011) Diagnosing errors in a land surface model (CABLE) in the time and frequency domains. *Journal of Geophysical Research: Biogeosciences (2005–2012)*, **116**, G01034

Wang Y-P, Zhang Q, Pitman AJ, Dai Y (2015) Nitrogen and phosphorous limitation reduces the effects of land use change on land carbon uptake or emission. *Environmental Research Letters*, **10**, 014001.

Waring BG, Adams R, Branco S, Powers JS (2015) Scale-dependent variation in nitrogen cycling and soil fungal communities along gradients of forest composition and age in regenerating tropical dry forests. *New Phytologist*,. doi:10.1111/nph.13654.

Wårlind D, Smith B, Hickler T, Arneth A (2014) Nitrogen feedbacks increase future terrestrial ecosystem carbon uptake in an individual-based dynamic vegetation model. *Biogeosciences*, **11**, 6131–6146.

Wieder WR, Bonan GB, Allison SD (2013) Global soil carbon projections are improved by modelling microbial processes. *Nature Climate Change*, **3**, 909–912.

Wieder WR, Cleveland CC, Smith WK, Todd-Brown K (2015) Future productivity and carbon storage limited by terrestrial nutrient availability. *Nature Geoscience*, **8**, 441–444.

Wright IJ, Westoby M (2003) Nutrient concentration, resorption and lifespan: leaf traits of Australian sclerophyll species. *Functional Ecology*, **17**, 10–19.

Yang X, Thornton PE, Ricciuto DM, Post WM (2014) The role of phosphorus dynamics in tropical forests – a modeling study using CLM-CNP. *Biogeosciences*, **11**, 1667–1681.

Zaehle S, Friedlingstein P, Friend AD (2010) Terrestrial nitrogen feedbacks may accelerate future climate change. *Geophysical Research Letters*, **37**, L01401.

Zaehle S, Medlyn BE, De Kauwe MG *et al.* (2014) Evaluation of 11 terrestrial carbon–nitrogen cycle models against observations from two temperate free-air CO_2 enrichment studies. *New Phytologist*, **202**, 803–822.

Supporting Information

Additional Supporting Information may be found in the online version of this article:

Appendix S1. CLM4.0 leaf litter N and retranslocated N calculation.

Appendix S2. The CLM4.0–FUN2.0-simulated passive N uptake.

Fig. S1. The annual mean (1995–2004) passive N uptake (g N m^{-2} yr^{-1}) simulated by CLM4.0–FUN2.0.

Fig. S2. The monthly mean (1995–2004) soil mineral N (g N m^{-2} month^{-1}) simulated by CLM4.0–FUN2.0.

Fig. S3. The annual mean (1995–2004) transpiration (mm yr^{-1}) simulated by CLM4.0–FUN2.0.

Appendix S3. The global distribution of C spent on N acquisition.

Fig. S4. The global mean annual (1995–2004) zonal distribution of the C used for N acquisition (Tg C yr^{-1}).

Fig. S5. The annual mean (1995–2004) C spent on N acquisition (g C m^{-2} yr^{-1}) simulated by CLM4.0–FUN2.0.

Appendix S4. Net primary productivity (NPP) variations in different biomes.

Fig. S6. The mean annual (1995–2004) zonal net primary productivity (NPP) variation fraction between CLM4.0 and CLM4.0–FUN2.0.

Fig. S7. The global mean annual (1995–2004) net primary productivity (NPP) per unit area (g C m^{-2} yr^{-1}) in deciduous broadleaf forest, grassland, evergreen needleleaf forest, deciduous needleleaf forest, evergreen broadleaf forest, and shrubland.

Fig. S8. The global mean annual (1995–2004) net primary productivity (NPP) (Pg C yr^{-1}) in deciduous broadleaf forest, grassland, evergreen needleleaf forest, evergreen broadleaf forest, deciduous needleleaf forest, and shrubland.

Appendix S5. The figures in Discussion.

Fig. S9. (a) The global nutrient-limitation product developed from remote sensing (Fisher *et al.*, 2012), and (b) the global mean annual (1995–2004) net primary productivity (NPP) down-regulation fraction between CLM4.0 and CLM4.0–FUN2.0.

Fig. S10. The regressed net primary productivity (NPP) variation with the nutrient limitation data discussed in *Fisher et al.* (2012) in: (a) C3 grassland (non-arctic) and (b) broadleaf evergreen tropical forest.

Fig. S11. The seasonality of N uptake (g N m^{-2} month^{-1}) at the Morgan Monroe (MM) site with doubled soil mineral N.

Fig. S12. CLM4.0 simulations at the Morgan Monroe (MM) site for (a) the leaf N storage pool (g N m^{-2} day^{-1}) and (b) the retranslocated N pool (g N m^{-2} day^{-1}).

Fig. S13. The normalized new leaf N storage pool in temperate deciduous forests. This new pool combines the leaf N storage pool and retranslocated N pool of CLM4.0.